Process modelling, design and technoeconomic evaluation for continuous paracetamol crystallisation

Anton Friedl, Jiří J. Klemeš, Stefan Radl, Petar S. Varbanov, Thomas Wallek (Eds.)
Proceedings of the 28th European Symposium on Computer Aided Process Engineering
June 10th to 13th, 2018, Graz, Austria.
https://doi.org/10.1016/B978-0-444-64235-6.50285-0

Process modelling, design and technoeconomic evaluation for continuous paracetamol crystallisation

Hikaru G. Jolliffe, Dimitrios I. Gerogiorgis*

School of Engineering (IMP), University of Edinburgh, Edinburgh, EH9 3FB, UK

D.Gerogiorgis@ed.ac.uk

Abstract

Continuous Pharmaceutical Manufacturing (CPM) has received significant research interest as a way to achieve a step-change in the performance of pharmaceutical production, where innovations are incremental at best due to the current paradigm – batch production – being a relatively mature technology. In this work, a Continuous Oscillatory Baffled Crystalliser (COBC) for paracetamol crystallisation has been modelled and optimal design and operation has been determined via nonlinear optimization (NLP). Clear trends emerge, with rate of antisolvent use having a marked impact of COBC volumes; crystal seed mass loading also has a strong effect. However, there are tradeoffs between mass efficiency, cost and volume, and product crystal size. The trends and optima illustrate how process modelling, simulation and optimisation provide clear insights into process performance and decisions on acceptable tradeoffs.

Keywords: Continuous Oscillatory Baffled Crystalliser (ODBC), paracetamol.

1. Introduction

Pharmaceutical production has long relied solely on batch processing, and while it has many benefits including equipment flexibility and the know-how of a mature technology, in an environment of growing R&D expenditure and a greater awareness of and a drive to be more sustainable, research interest has turned towards Continuous Pharmaceutical Manufacturing (CPM); continuous production can achieve higher yields purities, better heat and mass transfer, decreased processing times, and better efficiency and reliability. The need for cost-effective R&D methodologies brings process modelling and simulation to the forefront of initial stages of process option evaluation. Furthermore, they are also of great utility in evaluating alternative design parameters for existing or newly developed processes (Benyahia et al., 2012). Continuous crystallisation has received significant research attention toward developing separation technologies for CPM, with both stirred tanks and tubular crystallisers types studied in great detail (Ferguson et al., 2014; McGlone et al., 2015; Diab and Gerogiorgis, 2017).

In previous work, we have used modelling and simulation to economically evaluate two CPM processes, and we have also used nonlinear optimisation of these process models to determine optimal design and operating parameters for key product separation operations (Jolliffe and Gerogiorgis, 2017a, 2017b). In the present work, we systematically incorporate models for continuous crystallisation, published crystallisation kinetic data, and economic analysis into a nonlinear optimisation model

to determine optimal crystallisation operation and design for the recovery of an analgaesic Active Pharmaceutical Ingredient (API), paracetamol. This key API has been widely used as a model API for CPM studies, with published data on crystallisation kinetics available (Brown et al., 2015; Cruz et al., 2016). The impact of temperature, crystalliser size and configuration, antisolvent type and quantity, and flowrate are considered. The optimisation cases are formulated into a nonlinear optimisation model to determine optimal Continuous Oscillatory Baffled Crystalliser design variables and process conditions. Technical (API recovery), environmental (E-factor) and economic metrics (Capital Expenditure, CapEx) are used for comprehensive process evaluation.

2. Continuous Oscillatory Baffled Crystallisers (COBC)

Continuous Oscillatory Baffled Crystallisers (COBC) are a development of Oscillatory Baffled Reactors, and in essence are a series of baffles in long (i.e. high length-to-diameter ratio) tubes, and in appearance are similar to Plug Flow crystallisers with baffles.. COBC units tend to offer improved performance over the latter, as well as over batch crystallisers. They offer improved scaling, heat and mass transfer and decreased processing times (Lawton et al., 2009). COBC units operate by inducing an oscillatory flow in the fluid contents, and there is also a net flow through the unit (as this is a continuous process) which is independent of the oscillatory flow. The use of a reciprocating pump is a common way to generate the oscillatory flow: as the fluid moves back and forth across the baffles, the eddies generated enhance mixing and thus improve local crystallisation performance considerably. Baffle design primarily varies in terms of the orifice-to-internal diameter ratio, the gap between the baffles and the number of orifices in the baffles; in some cases constrictions are used instead of baffles.

3. Nonlinear optimisation and process model

The objective function to be minimized is a Capital Expenditure (*CapEx*) function (Eq. 1), from a capacity-power law using crystalliser volume. The coefficient a and exponent n were generated by fitting publicly available data for cost and capacity of commercial COBC units. Crystalliser volume is computed in a relatively straightforward manner (Eq. 2), from total volumetric throughput and the residence time required to achieve the desired objectives (such as yield). The population balance (Eq. 3) and mass balance (Eq. 4) are solved via a moment transformation (Eq. 5) (Brown et al., 2014). Key variables in (Eq. 5) include characteristic crystal length L (m), growth rate G (m s^{-1}). The volume shape factor k_v is taken to be 0.866, typical for the monoclinic Form I of paracetamol which is often encountered (Brown and Ni, 2011), and the crystal density ρ_{API} is 1.3 $g.cm^{-3}$. Nucleation is considered to be negligible, so the Br_o^j terms are ignored. Growth rate G is computed via the an empirical correlation (Eq. 6) (Brown and Ni, 2011), where ΔC_{API} is the degree of supersaturation (Eq. 7), $\dot{Q}_{AS}$ is the rate of antisolvent addition in mL min^{-1}, and the oscillatory flow Reynold Number Re_o (Eq. 9). In the latter term angular velocity $\omega = 2\pi f_{osc} a_{osc}$ (ms^{-1}) replaces the superficial fluid velocity found in the normal (Net Flow) Reynolds Number (Re_n, Eq. 9). Here, f_{osc} and a_{osc} are the frequency and amplitude of the fluid oscillation, respectively (normally taken to be 2 Hz and 10 mm in this model). In the literature, values for both Re_o and Re_n are suggested to achieve the best mixing, often above 300 for the former and above 50 for the latter. In this model we have imposed similar requirements, although with a higher Re_o; values over 4,000 are reported (Brown and Ni, 2011). The Re_o to Re_n ratio (ψ) has an optimal mixing interval; operation may vary outside reported ranges (Eq. 9) by as much as 10%.

The solubility of paracetamol in different solvent systems has been commonly studied in the literature. Here, the use acetone as process solvent is modelled, with either water or toluene as antisolvent. Empirical values for paracetamol were taken fitted high order polynomial surrogate equations to calculate solubilities (Eq. 8) (Fig. 1). With water use there is a solubility peak, and within a certain range adding water will in fact increase API solubility. To avoid this, the rate of antisolvent use was limited to a range of 50:50 to 20:80 by weight (process solvent acetone : antisolvent). It transpires that the use of toluene results in highly impractical residence times and volumes (very long/large), and so the results presented in this work refer to the use of water as an antisolvent.

Seed crystal loading can vary from 0.5% to 2.0% by weight (seed w.r.t. solvent and antisolvent). The following assumptions are made: a) seed crystals are monodisperse (i.e. of same size) and of monoclinic Form I; b) no nucleation, agglomeration or

$$\min CapEx = aV_{COBC}{}^{m} \tag{1}$$

s.t.

$$V_{COBC} = \dot{Q}_{Tot}\tau_{req} \tag{2}$$

$$\frac{\delta n}{\delta t} + G\frac{\delta n}{\delta L} = 0 \tag{3}$$

$$\frac{\mathrm{d}C_{API}}{\mathrm{d}t} = -3\rho_{API}k_v G\int_0^{\infty} L^2 n\,\mathrm{d}L \tag{4}$$

$$\mu_j = \int_0^{\infty} L^j f_n(L,t)dL, \qquad \begin{bmatrix} \dot{\mu}_0 \\ \dot{\mu}_1 \\ \dot{\mu}_2 \\ \dot{\mu}_3 \\ \dot{\mu}_{C_{API}} \end{bmatrix} = \begin{bmatrix} B \\ G\mu_0 + Br_0 \\ 2G\mu_1 + Br_0^2 \\ 3G\mu_1 + Br_0^3 \\ -\rho_{API}k_v(3G\mu_1 + Br_0^3) \end{bmatrix} \tag{5}$$

$$G \cdot 10^8 = 3.78 \cdot 10^{-12}\Delta C_{API}^{1.570}\dot{Q}_{AS}^{1.158}Re_o^{2.155} + 21.50 \tag{6}$$

$$\Delta C_{API} = C_{API} - C_{API}^{sat},\ S = \frac{C_{API}}{C_{API}^{sat}} \tag{7}$$

$$C_{API}^{sat} = \sum_{i=0}^{n}\sum_{j=0}^{k} a_{ij} m_{AS,\%}{}^{i} T^{j} \tag{8}$$

$$Re_o = \frac{2\pi f_{osc} a_{osc}\rho_{mix} d}{\mu_{mix}} > 1000,\ Re_n = \frac{\rho_{mix}u_{net}d}{\mu_{mix}} > 40,\ 10 > \psi = \frac{Re_o}{Re_n} > 4 \tag{9}$$

$$0.5 \le ASR \le 0.8 \tag{10}$$

$$0.5\frac{kg_{seed}}{kg_{solvent}} \le 100SMR \le 2.0\frac{kg_{seed}}{kg_{solvent}} \tag{11}$$

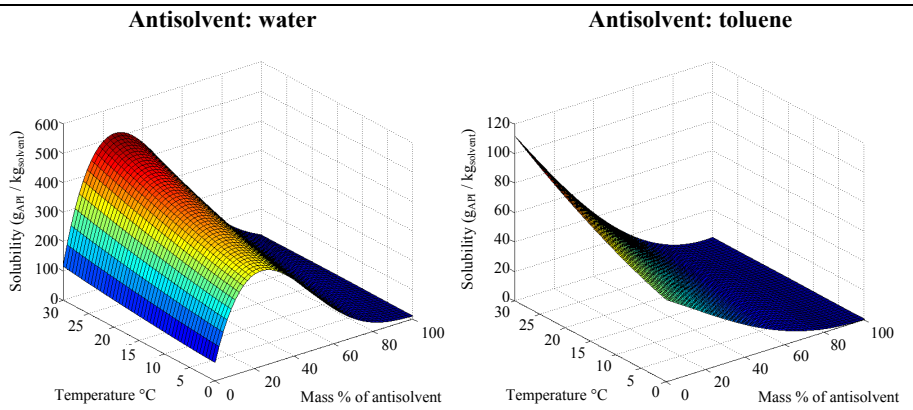

Figure 1. Paracetamol solubility in acetone-antisolvent mixtures (Granberg and Rasmuson, 2000).

breakage of crystals; c) crystal growth rates are size-independent; d) no impurities; e) sufficient heat transfer available to maintain a linear cooling profile. In terms of temperature, the inlet temperature can vary between 30 to 70 °C, and cooled to 5 °C; an inlet temperature of 50 °C is the default studied, and the other values investigated to see how optimality varies. Likewise, seed crystal size has been set at 40 microns by default, and larger sizes are investigated to study the optimal solution variation. Separate optimisation cases are formulated for varying inlet temperature and seed crystal size.

The MATLAB solver employed here is a constrained minimization routine (trust region reflective algorithm) with tolerances (stopping criteria) set to 10^{-6}. Gradients have been computed by the solver itself, and the solution time is reasonably fast, ranging between 30–100 seconds (the latter is the time required to generate capital expenditure response surfaces, while the time to run a single optimisation case is between 5–10 seconds). As stated, separate cases were formulated for initial temperatures. Separate cases were also performed for seed crystal sizes. A quick global search has been performed by checking convergence from multiple initial starting points; the runs always converged to the same point, and the absence of other local minima can be concluded with high confidence.

4. Results and discussion

Given a desired yield of 50%, the total cost response surface for an inlet temperature of 50 °C and a seed crystal size of 40 microns is given in Fig. 2A. The optimal solution (cost = 101,370 GBP) is pushed to bounds. It is evident that the rate of antisolvent use affects the total cost more significantly than the seed mass loading. Greater rates of antisolvent use result in lower costs via lower required residence times, due to faster growth rates. The tabulated values (Table 1) illustrate how the optimum changes with varying inlet temperatures, with a constant seed crystal size of 40 microns. Increasing the inlet temperature can drastically lower the cost via small required volumes and residence times. We can also see how the product crystal size varies, increasing with inlet temperature (and lowering with lower inlet temperature). This makes sense, as we assume the same initial supersaturation ratio (S = 1.5, Eq.7) in all cases: the higher the inlet temperature the higher the inlet solubility, thus higher supersaturation, thus greater API content, thus greater API precipitation for the same yield, thus larger product crystal sizes (as seed count is the same). Table 1 presents how capital cost, volume, residence time and product crystal size vary as a function of the seed crystal size used.

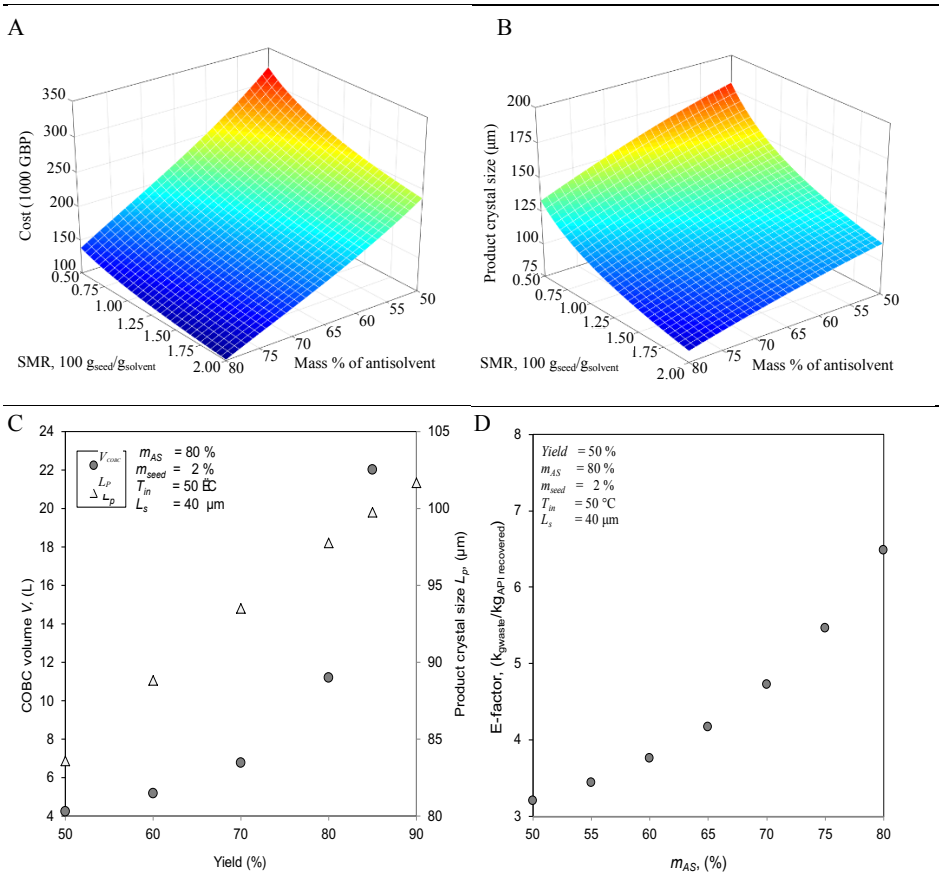

Figure 2. Total cost (A) and product crystal (B) response surfaces, volume and product size variation with required yield (C), and E-factor variation with antisolvent use (D).

For the same inlet temperature of 50 °C; optima variation is less pronounced as with different inlet temperatures. Of course, for a given seed mass loading, larger seed crystal sizes mean lower seed counts. The response surface for product crystal size is given in Fig. 2B. Lower antisolvent amount results in larger product crystals; again, this is an effect of seed count. With lower antisolvent amount, the mass of seed crystals added in absolute terms is less. Therefore, the seed count will lower, meaning crystals must grow more in order to achieve the same yield. The reason lower seed mass loading increases product size is similar. The change in required COBC volumes as a result of oscillation in the COBC unit is straightforward (values not shown): Higher angular velocities (ω, a combination of the oscillation frequency and amplitude) produce a clear trend of lower volumes; this is to be expected, as higher ω increases Re_o, which increases growth rates. Fig. 2C illustrates the variation of volumes and product crystal sizes for different required target yields (other results here are for a 50% yield). The inlet temperature is 50 °C, with a seed crystal size of 40 microns. Product crystal size increases linearly, while crystalliser volumes increase exponentially; achieving 90% yield is impractical.

Table 1. Optima variation for differing inlet temperatures (left) and seed crystal size (right).

Seed crystal size L_s = 40µm					*Inlet temperature* T_{in} = 50°C				
T_{in} (°C)	*CapEx* (10^3 £)	V_{COBC} (L)	τ_{req} (s)	L_p (µm)	L_s (µm)	*CapEx* (10^3 £)	V_{COBC} (L)	τ_{req} (s)	L_p (µm)
70	37.032	0.941	91	118.0	80	161.060	8.499	822	167. 2
60	60.337	1.954	189	99.2	70	147.280	7.435	719	146.3
50	101.370	4.250	411	83.6	60	132.970	6.380	617	125.4
40	170.600	9.265	896	71.5	50	117.700	5.315	514	104.5
30	283.530	19.822	1917	62.4	40	101.370	4.250	411	83.6

Finally, evaluating E-factors (mass of waste per unit mass of product; a measure of mass efficiency – lower is better) in Fig. 2D, we can see that for a given yield they worsen with increasing antisolvent quantity; E-factor is invariant with seed mass loading. However, with worsening E-factor, costs improve, highlighting the conflicting requirements in process design and evaluation, and the need for tradeoff decisions.

5. Conclusions

The solved optimisation cases illustrate the benefits and drawbacks of different combinations of solvent and antisolvent, in both technical and sustainability terms, and the varying impacts of inlet temperature, seed mass loading, seed crystal size, mechanical operation of the crystalliser, and rate of antisolvent use. For a desired yield of 50 %, the latter has the most significant effect on crystalliser cost (Capital Expenditure), while seed mass loading also has a strong effect. Higher required yields require exponentially larger and more costly crystallisers. The tradeoff between material efficiency (which has been calculated by means of the E-factor metric), and volumes and cost, underscores competing objectives that frequently arise during process design.

6. Acknowledgements

Mr. Hikaru G. Jolliffe gratefully acknowledges the financial support of the Engineering and Physical Sciences Research Council (EPSRC) via a Doctoral Training Partnership (DTP) PhD fellowship awarded by the University of Edinburgh (EP/M506515/1).

References

Benyahia, B. et al., 2012. *Ind. Eng. Chem. Res.* 51, 15393–15412.
Brown, C.J. et al., 2015. *Chem. Eng. Process. Process Intensif.* 97, 180–186.
Brown, C.J. et al., 2014. *CrystEngComm* 16, 8008–8014.
Brown, C.J., Ni, X., 2011. *Cryst. Growth Des.* 11, 719–725.
Cruz, P. et al., 2016. *CrystEngComm* 18, 9113–9121.
Diab, S., Gerogiorgis, D.I., 2017. *Org. Process Res. Dev.* 21, 924–926.
Ferguson, S. et al., 2014. *Cryst. Growth Des.* 14, 617–627.
Granberg, R.A. and Rasmuson, A.C., 2000. *J. Chem. Eng. Data*, 45, 478–483.
Hodges, P., 2015. http://www.nitechsolutions.co.uk, accessed 9/11/2017.
Jolliffe, H.G., Gerogiorgis, D.I., 2017a. *Ind. Eng. Chem. Res.* 56, 4357–4376.
Jolliffe, H.G., Gerogiorgis, D.I., 2017b. *Comput. Chem. Eng.* 103, 218–232.
Lawton, S. et al., 2009. *Org. Process Res. Dev.* 13, 1357–1363.
McGlone, T. et al., 2015. *Org. Process Res. Dev.* 19, 1186–1202.